Journal of Bio- and Tribo-Corrosion (2020) 6:127
https://doi.org/10.1007/s40735-020-00425-z

Synthesis of Novel Gemini Surfactants Based on Succinic Acid and Their Application as Inhibitors for Carbon Steel Corrosion

Mona A. El-Etre[1] · Samar Abdelhamed[2] · Mohamed Deef Allah[2]

Received: 12 May 2020 / Revised: 17 August 2020 / Accepted: 11 September 2020 / Published online: 22 September 2020
© Springer Nature Switzerland AG 2020

Abstract
Three nonionic Gemini surfactants were synthesized based on succinic acid. The structures of the synthesized surfactants were characterized using FTIR and ^{1}H NMR spectra. The physical properties such as surface tension (γ), critical micelle concentration (CMC), surface pressure (effectiveness) (π_{CMC}), maximum surface excess concentration (Γ_{max}), and minimum surface area occupied by one molecule (A_{min}) were calculated. The inhibitive power of the surfactants toward acid corrosion of carbon steel was obtained using weight loss and electrochemical techniques. The morphology of the carbon steel surface was examined by atomic force microscope. It was found that all the three surfactants act as good inhibitors for steel corrosion in the acidic medium. The inhibition efficiency increases with increasing surfactant concentration and exposure time. The inhibition action was attributed to the adsorption of the surfactant's molecules on the steel surface. It was found that the adsorption process is spontaneous and obeys Langmuir adsorption isotherm. A mechanism was proposed for the inhibition action based on the obtained results.

Keywords Organic synthesis · Gemini surfactant · FTIR · NMR · C-steel · Corrosion inhibition

1 Introduction

During the cleaning of petroleum pipelines and tanks from scales by hydrochloric acid, serious corrosion could occur. Such a process leads to huge economic loss due to the loss of metal and maybe the contained materials as well. Therefore, the addition of corrosion inhibitors to the pickling acid solution is essential to avoid such loss.

Organic inhibitors are known to act through adsorption on the metal surface as an isolating film between the corrosive medium and the metal [1–15]. The organic inhibitor is oriented toward the metal surface under the influence of electrostatic attraction. The process is favored further due to some extra features in the compound structure. Among these features, the charges carried by the compound, the electron density, the presence of unsaturated bonds, and lone pairs of electrons have significant importance [16].

Much work was done on tens of surfactant compounds as potential corrosion inhibitors [17–21]. Surfactants showed promising results as highly efficient corrosion inhibitors. This is because of their unique features in their structure as well as their natural affinity to adsorb at the interface. Recently, there is extensive work on the examination of Gemini surfactants as corrosion inhibitors. Gemini surfactants with their special structure consist of two chains separated by spacer and are expected to act as corrosion inhibitors better than the usual monomeric surfactants. Many pieces of the research reported a very good impact of such surfactants as inhibitors for many metals and alloys in different aggressive media. The high inhibition efficiency was attributed to the special molecular structure of this category of surfactants [22–26].

In the present work, three of Gemini surfactants were synthesized, characterized, and tested as inhibitors for carbon steel corrosion, used in the petroleum industry, in HCl solution. Weight loss measurements and electrochemical

Electronic supplementary material The online version of this article (https://doi.org/10.1007/s40735-020-00425-z) contains supplementary material, which is available to authorized users.

✉ Mona A. El-Etre
mona.eletr@bhit.bu.edu.eg

[1] Basic Science Department, Faculty of Engineering, Benha University, Benha, Egypt

[2] Basic Science Department, Faculty of Engineering, Benha University, Shoubra, Egypt

polarization technique were used for the determination of the inhibitive action of the surfactants.

2 Experimental

2.1 Materials

Succinic acid was obtained from Across Chemical Company (UK). 1, 4 Butanediol, diethanolamine and propylene oxide were purchased from Sigma-Aldrich (Germany). Thionyl chloride and P-toluene sulfonic acid were obtained from Fluka Chemika (Germany). Potassium hydroxide and all solvents (benzene and xylene) were dried and supplied by (Al-Gomhuria Trade Pharmaceuticals and Chemical Company, Cairo, Egypt).

2.2 Synthesis of 3-{[6-(2-Carboxyethoxy)-6-oxohexanoyl]oxy} propanoic Acid

The diester compound 3-{[6-(2-carboxyethoxy)-6-oxohexanoyl]oxy} propanoic acid was prepared by refluxing a mixture of 1,4 butandiol (0.05 mol) with succinic (0.1 mol), respectively, in 50 ml of dry benzene for 6 h, in presence of 0.1 wt% *p*-toluenesulfonic acid as a catalyst. After cooling reaction mixture, distilled water was added. The benzene layer containing the diester was separated. The ester solution was dried overnight and then vacuum distilled to obtain the crude product. Further purification was affected by fractional distillation under vacuum [27].

2.3 Synthesis of 1,6-Bis(3-chloro-3-oxopropyl) hexanedioate

Thionyl chloride(0.1 mol) was added to the product of the first step by dropwise addition to the corresponding diester compound 1,6-bis(3-chloro-3-oxopropyl) hexanedioate (0.05 mol) for 3 h in water bath [28].

2.4 Synthesis of 1,6-Bis({2-[bis(2-hydroxyethyl) carbamoyl]ethyl}) hexanedioate

The diester dichloro compound 1,6-bis(3-chloro-3-oxopropyl) hexanedioate reacted with diethanolamine in 50 ml xylene at the reaction molar ratio 0.5:1.0 by dropwise addition of triethylamine (TEA) as a catalyst under refluxing for 5 h at 120 °C. The product was extracted by petroleum ether [29].

2.5 Synthesis of Nonionic Gemini Surfactants

0.5 Wt% KOH solution containing 0.01 mol of the prepared (diester diamino compound) formed in the third step was stirred and heated to 70 °C while passing a slow stream to nitrogen through the system to flush out oxygen. The nitrogen stream was stopped, and propylene oxide was added dropwise with continuous stirring and heating under an efficient reflux system to retain the propylene oxide. The reaction was conducted for different intervals of time ranging from 1 to 10 h. The system was then loaded up with nitrogen and cooled. The reactor vessel was weighed. The measure of responded propylene oxide and the normal level of propoxylation were resolved from the augmentation in the mass of the response blend [30, 31] with molar ratio 5, 10, and 15, respectively, to obtain the synthesized nonionic Gemini surfactants as shown in Fig. 1.

2.6 Measurements

2.6.1 Surface Tension

Surface tension measurements were obtained using a De-NoüyTensiometer (Kruss-K6 type; Germany) with a platinum ring device. Freshly prepared aqueous solutions of the synthesized surfactants in deionized water within the concentration range of 0.01–0.00001 M were tested at 25 °C. The ring was washed twice after each reading, first by ethanol and then by distilled water. The apparent surface tension was measured 5 times for each sample within a 2-min interval between each reading [32].

2.6.2 Critical Micelle Concentration (CMC) Measurements

The CMC concentration relates to where the surfactant first shows the most reduced surface tension and after which it remains almost steady. The CMC esteems were obtained through a customary plot of the surface tension versus the logarithm of the convergence of surfactant at room temperature (25 °C). The relation between surface tension and concentration of the three tested surfactants is in the Supplementary Material (Fig. S1).

2.6.3 Corrosion Rate Measurements

2.6.3.1 Weight Loss Measurements The concentration of the HCl utilized as a forceful medium was balanced by titration against a standard solution of sodium carbonate. Each test has been led three times and the average weight reduction of them was recorded. The inhibition efficiency (η) and

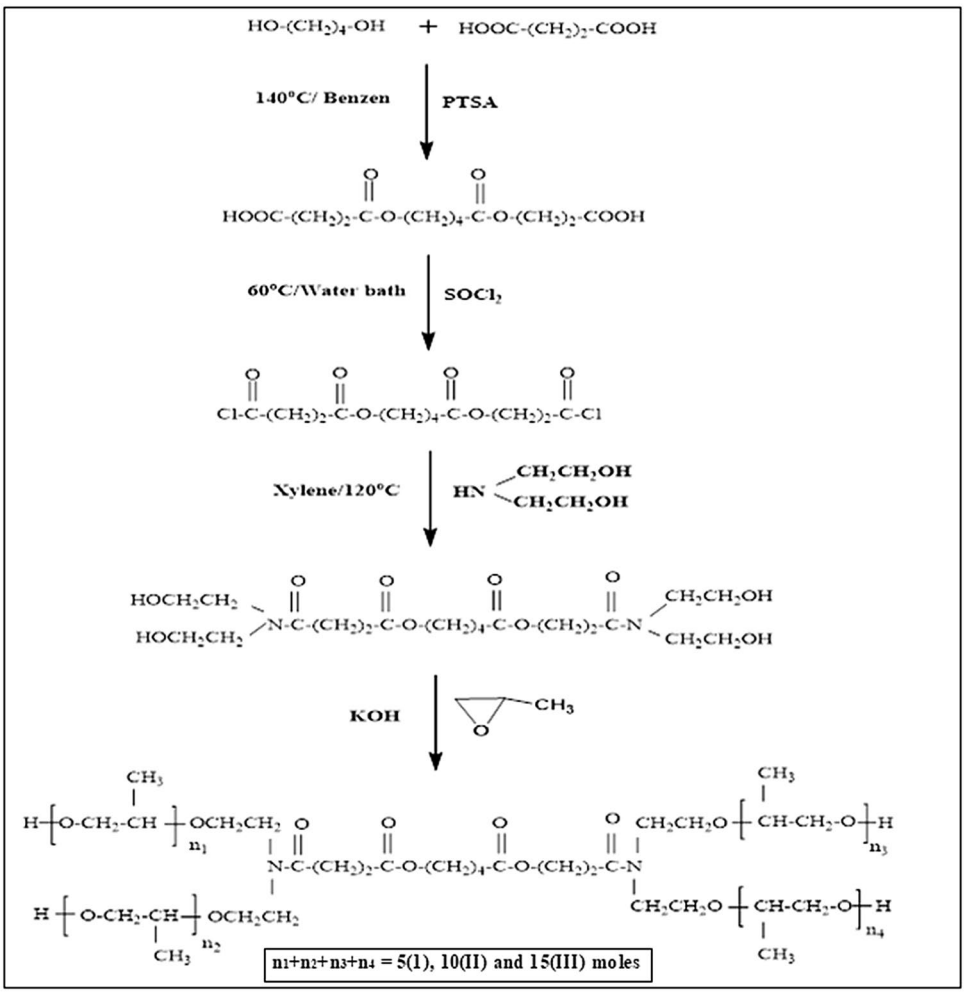

Fig. 1 Synthesis procedure of nonionic Gemini surfactants

the fraction of surface covered by the additive (θ) were calculated using the following equations, respectively:

$$\eta = \left(\frac{W_f - W_i}{W_f}\right) \times 100, \quad (1)$$

$$\theta = \left(\frac{W_f - W_i}{W_f}\right), \quad (2)$$

where W_f and W_i are weight loss in free and inhibited solutions, respectively.

2.6.3.2 Electrochemical Polarization The electrochemical investigations were ran utilizing a three-electrode cell, with a platinum counter terminal and saturated calomel electrode (SCE) as a reference electrode. The carbon steel working electrode was a rode impeded in a glass tube with Araldite leaving an exposed bottom side with an area of 0.1 cm^2. The uncovered surface was rubbed with various grades of emery papers, flushed with refined water and acetone, then dried between two filter papers, before embedding in the test arrangement. The electrode was lifted in the test solution until it reaches a steady-state potential value before starting the measurements. Corrosion parameters were measured using Metrohm potentiostat supported with Nova software for calculations. The potentiodynamic polarization measurements were obtained using a scan rate of 1.0 mV s^{-1} at 25 ± 1 °C. The inhibition efficiency (η) obtained from electrochemical polarization was calculated using the following equation:

$$\eta = \left(\frac{I_f - I_i}{I_f}\right) \times 100, \quad (3)$$

where I_f and I_i are corrosion current density for the free and inhibited solutions, respectively.

2.6.3.3 Surface Examination The morphology of the carbon steel surface was examined by atomic force microscopy (AFM; Pico SPM-Picoscan 2100, Molecular Imaging, Arizona, AZ, USA). Carbon steel coupons were analyzed after three hours of exposure time to 1.0 M HCl

solutions in the absence and presence of 10^{-3} M of surfactants (I–III).

3 Results and Discussion

3.1 FTIR Spectra

The structures of 3-{[6-(2-carboxyethoxy)-6-oxohexanoyl] oxy}propanoic acid show absorption bands at 3355 cm^{-1} assigned to the (OH) group, 2956 and 2914 cm^{-1} ascribed to CH aliphatic, 1730 cm^{-1} assigned to C=O of the ester group, 1471 cm^{-1} C–H bond of CH_2 group, and 1158 cm^{-1} ascribed to stretching of C–O group (see Supplementary Material Fig. S2).

The structures of 1,6-bis(3-chloro-3-oxopropyl) hexanedioate show absorption bands at 2955 and 2926 cm^{-1} ascribed to CH aliphatic, 1733 cm^{-1} assigned to C=O of the ester group, 1435 cm^{-1} C–H bond of CH_2 group, and 1164 cm^{-1} ascribed to stretching of C–O group (see Supplementary Material Fig. S3).

The structures of 1,6-bis({2-[bis(2-hydroxyethyl)carbamoyl]ethyl}) hexanedioate show absorption bands at 3258 cm^{-1} assigned to (OH) group, 2925 cm^{-1} ascribed to CH aliphatic, 1730 cm^{-1} assigned to C=O of the ester group, 1567 cm^{-1} assigned to stretching of C=O, 1446 cm^{-1} C–H bond of CH_2 group, and 1186 cm^{-1} ascribed to stretching of C–O group (see Supplementary Material Fig. S4).

The structures of the synthesized nonionic Gemini surfactants were elucidated using FTIR spectra. The FTIR spectrum of synthesized surfactants (I) (Fig. 2a) show absorption bands at 3348 cm^{-1} assigned to (OH) group, 2969 cm^{-1} ascribed to CH aliphatic, 1733 cm^{-1} assigned to C=O of

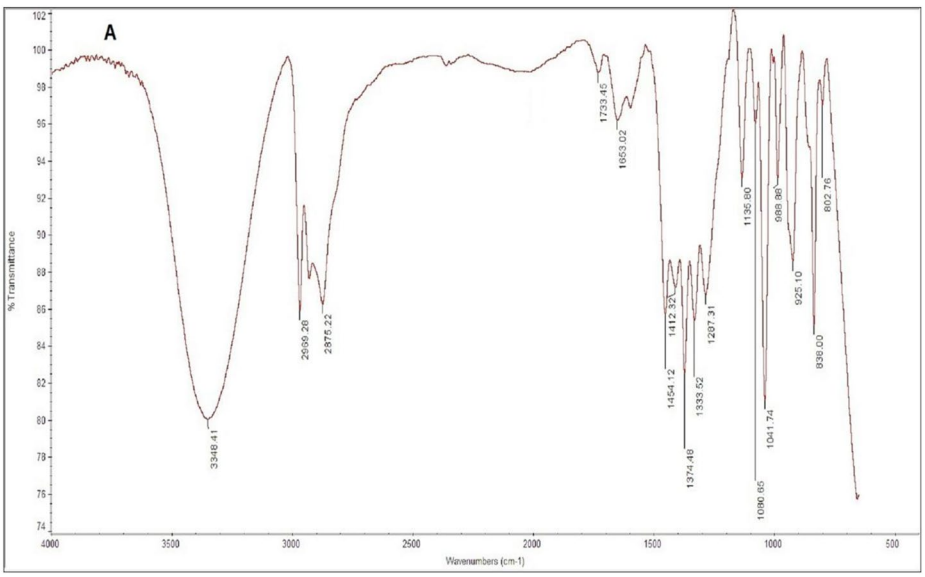

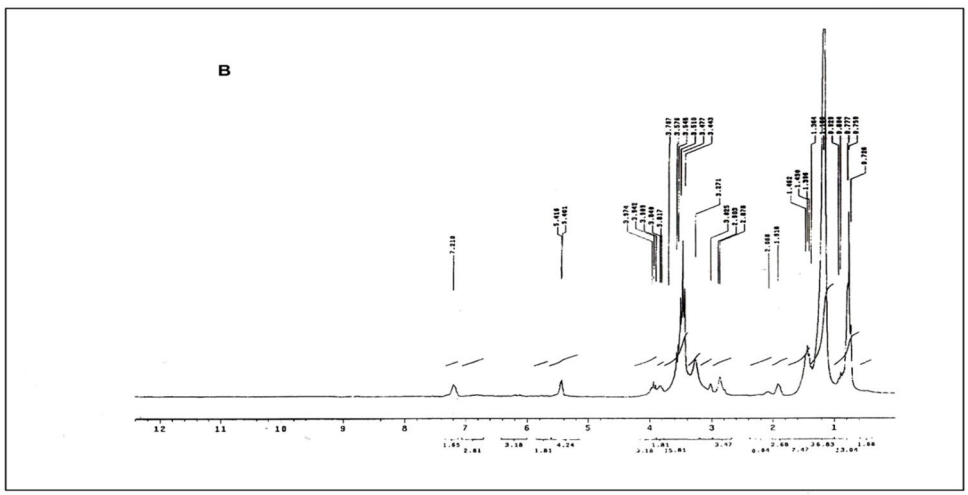

Fig. 2 **a** FTIR spectra of (I) and **b** ^{1}H NMR of (I) nonionic Gemini surfactants

the ester group, 1454 cm^{-1} C–H bond of CH_2 group, and 1080 cm^{-1} ascribed to C–O–C of ether group.

The FTIR spectrum of synthesized surfactants (II) show absorption bands at 3376 cm^{-1} assigned to (OH) group, 2915 cm^{-1} ascribed to CH aliphatic, 1722 cm^{-1} assigned to C=O of the ester group, 1474 cm^{-1} C–H bond of CH_2 group, and 1088 cm^{-1} ascribed to C–O–C of ether group (see Supplementary Material Fig. S5).

The FTIR spectrum of the synthesized surfactants (III) show absorption bands at 3346 cm^{-1} assigned to (OH) group, 2927 cm^{-1} ascribed to CH aliphatic, 1729 cm^{-1} assigned to C=O of the ester group, 1456 cm^{-1} C–H bond of CH_2 group, and 1088 cm^{-1} ascribed to C–O–C of ether group(see Supplementary Material Fig. S6).

3.2 ^{1}H NMR Spectra

The ^{1}H NMR (DMSO-d_6) spectrum of the synthesized nonionic Gemini surfactants (I) (Fig. 2b) show different peaks at $\delta = 0.853$ ppm (t, 12H of $–CH_3$); $\delta = 1.024$ ppm [m, 8H of $2(CH_2)_2$]; $\delta = 1.244$ ppm (m, 8H of N–CH_2); $\delta = 2.5$ ppm (t, 8H of CH_2–O–C=O); $\delta = 3.191$–3.578 ppm (m, 12H of repeated propylene oxide units); and $\delta = 7.210$ ppm (broad S, 4H of OH).

The ^{1}H NMR (DMSO-d_6) spectrum of the synthesized nonionic Gemini surfactants (II) show different peaks at $\delta = 0.969$ ppm (t, 12H of $–CH_3$); $\delta = 1.025$ ppm [m, 8H of $2(CH_2)_2$]; $\delta = 2.503$ ppm (t, 8H of CH_2–O–C = O); $\delta = 3.145$–3.525 ppm (m, 12H of repeated propylene oxide units); and $\delta = 7.205$ ppm (broad S, 4H of OH) (see Supplementary Material Fig. S7).

The ^{1}H NMR (DMSO-d_6) spectrum of the synthesized nonionic Gemini surfactants (III) show different peaks at $\delta = 0.098$ ppm (t, 12H of $–CH_3$); $\delta = 1.049$ ppm [m, 8H of $2(CH_2)_2$]; $\delta = 1.232$ ppm (m, 8H of N–CH_2); $\delta = 2.501$ ppm (t, 8H of CH_2–O–C = O); $\delta = 3.206$–3.353 ppm (m, 12H of repeated propylene oxide units); and $\delta = 7.490$ ppm (broad S, 4H of OH) (see Supplementary Material Fig. S8).

3.3 Surface Active Properties

The surface tension (γ) values and critical micelle concentration (CMC) obtained for different concentrations of the aqueous solution of the synthesized nonionic Gemini surfactants at 25 °C are listed in Table 1. The value of surface pressure (effectiveness) (π_{CMC}), maximum surface excess concentration (Γ_{max}), and minimum surface area (A_{min}) were calculated using Eqs. (4)–(6) [33–37].

$$\pi_{CMC} = \gamma_0 - \gamma_{CMC}, \tag{4}$$

where (γ_0) is the surface tension of pure water and (π_{CMC}) is the surface tension of the surfactant solution at the critical micelle concentration.

$$\Gamma_{max} = \frac{-1}{RT}\left(\frac{\delta\gamma}{\delta \ln C}\right), \tag{5}$$

where $\delta\gamma$ is surface pressure in mN/m, C is surfactant concentration, and $(\delta\gamma/\delta \ln C)_T$ is the slope of a plot of surface tension versus concentration curves below CMC at a constant temperature.

$$A_{min} = 10^{16}/\Gamma_{max}N, \tag{6}$$

where N is the Avogadro's number 6.023×10^{23}.

π_{CMC}, Γ_{max} and A_{min} values of the nonionic Gemini surfactants are listed in Table 1. From the data listed in Table 1, it is obvious that the CMC values decrease with increasing the molecular weight and number of propylene oxide units. Therefore, the number of molecules required for micelle formation decreases as a result of increasing size and due to the coiling of the surfactant's molecule. The increasing of surface tension at the critical micelle concentration (CMC) leads to a decrease in surfactant effectiveness. A substance that lowers the surface energy is, thus, present in excess at or near the surface, i.e., when the surface tension decreases with increasing activity of a surfactant. It was found that the A_{min} value of nonionic Gemini surfactants increases in the order: I < II < III. This sequence is consistent with the number of propylene oxide units present in the compound. Thus, as the length of the surfactant chain increases, due to the increase in propylene oxide units, the A_{min} increases. This result suggests a horizontal orientation of the surfactant molecules on the interface.

3.4 Corrosion Measurements

3.4.1 Weight Loss Measurements

The corrosion rate and inhibition efficiency values for the corrosion of carbon steel in 0.1 M HCl solutions free and

Table 1 Surface properties of the synthesized nonionic Gemini surfactants

A_{min} (nm^2/molecule)	$\Gamma_{max} \times 10^{-10}$ (mol/m^2)	CMC (mol/L)	π_{CMC} (mN/m)	γ_{CMC} (mN/m)	γ (mN/m) 0.1 wt% 25 °C	Compounds
15.8	10.49	0.0100	41	31	29.5	I
17.2	9.648	0.1570	40	32	31.0	II
18.5	8.94	0.1653	39	33	32.5	III

containing different concentrations of the three synthesized surfactants at different exposure times are presented in Table 2. Inspection of the table reveals that all the three surfactant compounds act as good inhibitors for the acid corrosion of carbon steel.

The relationship between the inhibition efficiency and surfactant (I) concentration, at different exposure times, is shown in Fig. 3. Similar curves were obtained for compounds (II and III) and presented in the Supplementary Materials (Figs. S9, S10). The curves of Fig. 3 show that the inhibition efficiency increases with increasing the surfactant concentration. It is of interest to note from the figures that the inhibition efficiency increases markedly upon increasing concentration up to a specific concentration of 10^{-4} M. Increasing surfactant concentration beyond this value has

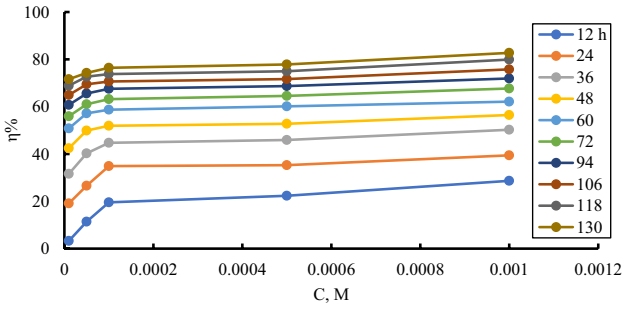

Fig. 3 Relationship between inhibition efficiency and compound (I) concentrations at different exposure times

Table 2 Corrosion parameters of C-steel in free and inhibited 0.1 M HCl solutions as obtained from the weight loss measurement

t (h)	Free	10^{-5} M		5×10^{-5} M		10^{-4} M		5×10^{-4} M		10^{-3} M	
	r	*R*	*η*	*r*	*η*	*r*	*η*	*r*	*η*	*r*	*η*
I											
12	0.514	0.497	3	0.455	11	0.413	19	0.399	22	0.366	29
24	0.614	0.496	19	0.451	27	0.400	35	0.397	35	0.372	39
36	0.723	0.494	31	0.432	40	0.399	45	0.391	46	0.359	50
48	0.822	0.473	42	0.411	50	0.395	52	0.3882	53	0.357	56
60	0.955	0.470	51	0.409	57	0.394	59	0.381	60	0.349	62
72	1.062	0.468	56	0.414	61	0.391	63	0.376	64	0.343	68
94	1.188	0.466	61	0.409	65	0.385	67	0.371	69	0.333	72
106	1.3015	0.456	65	0.397	69	0.382	71	0.368	72	0.315	76
118	1.447	0.450	69	0.395	73	0.379	74	0.362	75	0.291	80
130	1.6078	0.4562	712	0.4140	74	0.3787	76	0.3566	77	0.277	82
II											
12	0.514	0.395	23	0.312	39	0.259	49	0.255	50	0.245	52
24	0.614	0.395	36	0.310	49	0.259	58	0.253	59	0.243	60
36	0.723	0.394	45	0.310	57	0.257	64	0.253	65	0.242	66
48	0.822	0.394	52	0.308	62	0.257	69	0.252	69	0.242	70
60	0.955	0.393	59	0.308	68	0.256	73	0.251	74	0.241	75
72	1.062	0.393	63	0.307	71	0.256	76	0.251	76	0.239	77
94	1.188	0.393	67	0.308	74	0.255	78	0.250	79	0.237	80
106	1.301	0.392	70	0.308	76	0.255	80	0.248	81	0.235	82
118	1.447	0.392	73	0.307	79	0.254	82	0.248	83	0.233	84
130	1.607	0.391	752	0.307	80	0.254	84	0.247	840	0.216	86
III											
12	0.514	0.436	15	0.359	30	0.233	55	0.182	64	0.147	71
24	0.614	0.413	33	0.357	42	0.221	64	0.176	71	0.139	77
36	0.723	0.400	45	0.352	51	0.221	69	0.171	76	0.138	81
48	0.822	0.384	53	0.341	58	0.210	74	0.165	80	0.137	83
60	0.955	0.378	60	0.335	65	0.198	79	0.152	84	0.136	86
72	1.062	0.361	66	0.310	71	0.193	82	0.150	86	0.135	87
94	1.188	0.333	72	0.277	77	0.182	85	0.143	88	0.135	89
106	1.301	0.298	77	0.243	81	0.176	86	0.140	89	0.134	90
118	1.447	0.269	81	0.223	84	0.160	89	0.135	91	0.133	91
130	1.607	0.245	85	0.214	87	0.154	90	0.132	92	0.132	92

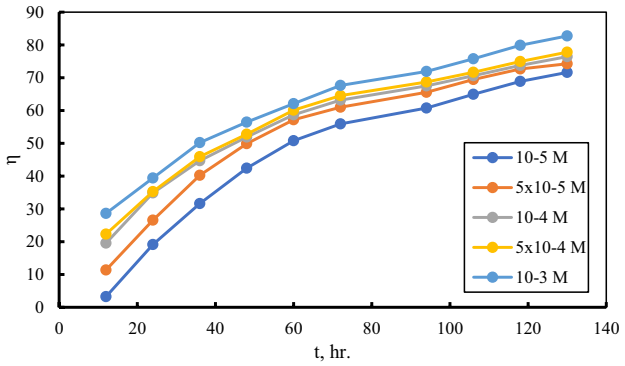

Fig. 4 Relationship between inhibition efficiency of different compound I concentrations and exposure time

a much smaller effect on the inhibition efficiency. The surfactants act as corrosion inhibitors through adsorption of their molecules on the steel surface forming a film that isolates the steel from the corrosive medium. In the present work, the surfactants approach their maximum inhibition capacity with such a very small concentration. This means that a small number of the surfactant molecules are enough to cover mostly of the metal surface. Thus, it is expected that the surfactant molecules adsorb on the metal surface, so as they cover the largest possible surface of the steel. This situation could be possible only if the molecules are adsorbed horizontally.

Figure 4 represents the relation between inhibition efficiency and exposure time for surfactant (I). Similar figures were also obtained for the other two surfactants and presented in the Supplementary Materials (Figs. S11, S12). It could be seen in the figure that the inhibition efficiency increases with increasing exposure time. This result suggests that the surfactant molecules need a period to orient themselves correctly to the proper surface sites for adsorption. Therefore, the number of adsorbed molecules increases with time, and consequently the inhibition efficiency increases.

The increment manner of inhibition efficiency is somewhat higher during the sixty hours of exposure, especially at low concentration. After this exposure period, there is a small drop in the increasing rate of inhibition efficiency. This result could be attributed to the high number of surface sites available for adsorption at the beginning of the exposure. However, as time goes on, the number of the occupied sites increases due to adsorption, and thus, the sites free for adsorption decrease. This situation diminishes the acceleration of inhibition efficiency.

3.4.2 Potentiodynamic Polarization Technique

Cathodic and anodic curves of C-steel polarization in 1.0 M HCl solutions devoid of and containing different

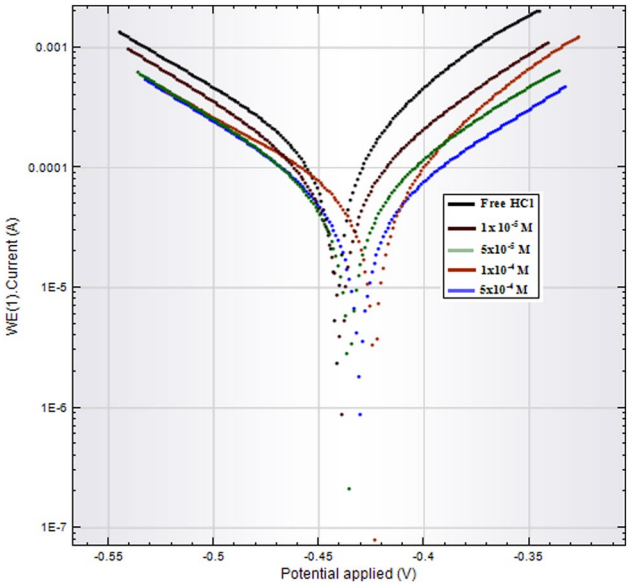

Fig. 5 polarization curves of C-steel in free and inhibited 1.0 M HCl solutions

concentrations of compound (I) are traced and represented in Fig. 5. Similar figures for the other two compounds are provided in the Supplementary Materials (Figs. S13, S14). It could be seen in all obtained figures that the curves behave in the same manner. Thus, the curves shift to lesser current densities and toward fewer negative potentials upon increasing the additive concentration. This result reflects the inhibitive power of the tested surfactant toward C-steel acid corrosion. The corrosion parameters extracted from the polarization curves are listed in Table 3. It is clear from the data of Table 3 that the corrosion potential increases with increasing surfactant concentration. However, the extent of corrosion potential variation is not enough to consider the additives as anodic inhibitors. Therefore, this result indicates that the surfactants act as mixed-type inhibitors. In agreement with this suggestion comes the dependence of Tafel constants on the surfactant concentration. It is obvious that the values of both anodic and cathodic Tafel constants do not change markedly in the presence of surfactant.

3.5 Adsorption Behavior

There is a general agreement that the first step in the corrosion inhibition process is the adsorption of inhibitor molecules on the metal surface. Such a process leads to the formation of isolating film that prevents the mass and charge transfer between the metal and its environment. The nature of the adsorption process could be fairly described by its adsorption isotherm. Many adsorption isotherms were tested for the data obtained from weight loss experiments. It was found that Langmuir adsorption isotherm is the most fitted

Table 3 Polarization parameters of C-steel corrosion in 1.0 M HCl solutions free and containing different concentrations of compounds (I–III)

Concentration (M) × 10^5	$-E_{corr}$ (mV)	B_a (mV/decade)	$-\beta_c$ (mV/decade)	I_{corr} (μA/cm^2)	η
Free	448	90	85	306.36	
I					
5	439	105	62	37.60	87.90
10	432	106	76	34.58	88.71
50	425	121	65	32.40	89.42
II					
1	422	94	64	47.00	84.66
5	412	109	66	32.96	89.24
10	401	114	70	25.42	91.70
50	401	138	72	21.14	93.10
III					
1	434	81	78	40.91	86.65
5	436	91	95	26.23	91.44
10	435	101	95	21.56	92.96
50	432	107	92	20.47	93.32

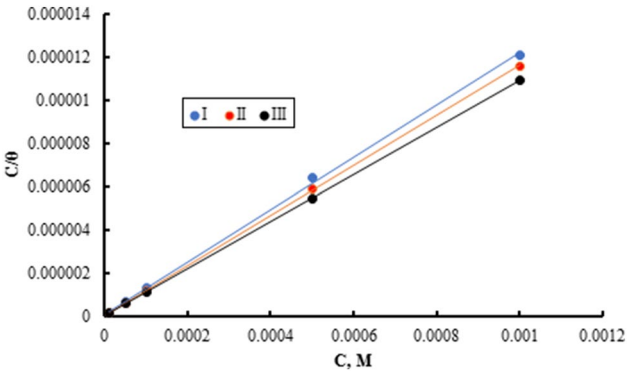

Fig. 6 Langmuir isotherm for the tested compounds

with the obtained data. Langmuir adsorption isotherm is defined by the equation:

$$\frac{C}{\theta} = \frac{1}{K_{ads}} + C, \tag{7}$$

where C is the inhibitor concentration, θ is the fraction of the surface covered by the adsorbed molecules, and K_{ads} is the equilibrium constant of the adsorption process. The equilibrium constant of the adsorption process is related to the standard free energy of adsorption by the equation:

$$\ln K = \ln \frac{1}{55.5} - \frac{\Delta G^{o}_{ads}}{RT}. \tag{8}$$

The value of 55.5 stands for the molar concentration of water.

Figure 6 represents the plots of C against C/θ for the three tested surfactants. Straight lines with unit slopes were obtained confirming the fellowship to the Langmuir isotherm. Therefore, according to this isotherm, the free energy of adsorption is independent of the covered area of the surface. Moreover, there must be no interaction between the adsorbed molecules. The obtained values of the standard free energy of adsorption are tabulated in the Table 4. The negative sign indicates the spontaneity of the adsorption process. It is of interest to note that the values of ΔG^{o}_{ads} are around 40 kJ/mol. Such a case suggests a chemical adsorption mechanism. On the other hand, the value increases in the order I < II < III. This sequence reflects the affinity of the surfactant molecules to adsorb on the steel surface.

Table 4 Values of free energy of adsorption

Surfactant	$-\Delta G^{o}_{ads}$(kJ/mol)
I	39.89
II	41.60
III	43.88

3.6 Atomic Force Microscopy (AFM)

Atomic force microscopy (AFM) is an investigation tool which gives details about the surface topography. The use of such a technique is useful for corrosion researches since it provides much information about the roughness of the examined surface. Both two and three diminution's images of the carbon steel surface after exposure to 1.0 M HCl free and inhibited with 10^{-3} M of the three tested surfactants are represented in Fig. 7. The full-sized images could be found in the Supplementary Materials (Figs. S15, S16, S17, S18, S19, S20, S21, S22). Inspection of the images in the figure reveals that the roughness of the carbon steel surface is

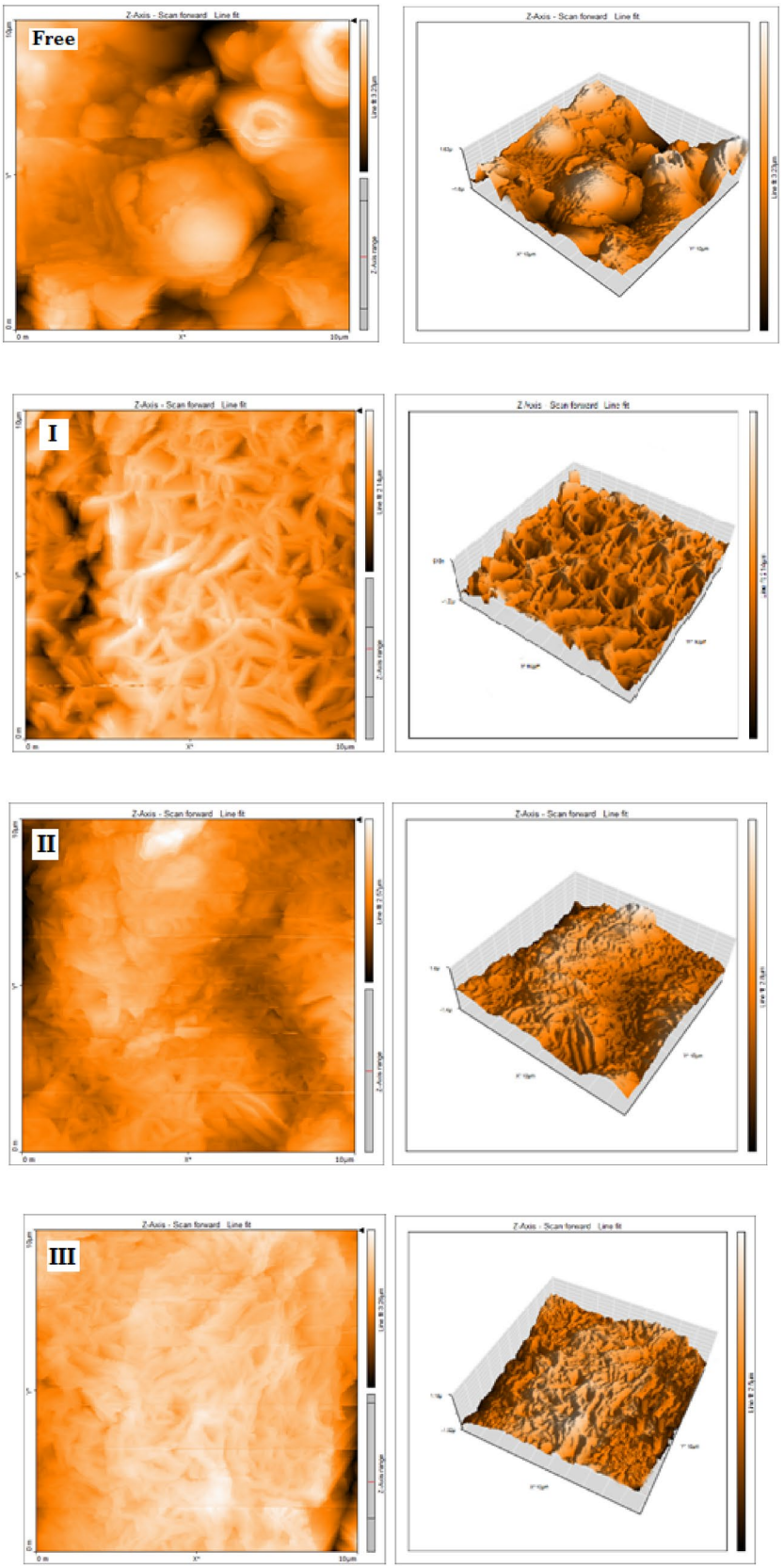

Fig. 7 2D and 3D atomic force images of the carbon steel surface in free and inhibited 1.0 M HCl solutions

highly reduced due to the presence of the tested surfactants. The roughness decreases depending on the type of additives in the order of I > II > III.

Table 5 presents the roughness data of the carbon steel samples after exposure to solutions of 1.0 M HCl containing 1×10^{-3} M of each of the three tested surfactants for 1 day at 25 °C. Table contains the roughness average (S_a), the peak height (S_p), and the valley depth (S_v). The data in Table 5 show that all the measured values decrease going from free acid solution to the inhibited one according to the sequence free > I > II > III. It is obvious that the carbon steel surface becomes smoother upon the addition of any of the three tested surfactants. This effect is attributed to the adsorption of the surfactant molecules on the carbon steel surface. Thus, the effectiveness of the surfactants increases in the same order of inhibition efficiency obtained by the above technique: III > II > I. This sequence is the same as that obtained from weight loss and electrochemical techniques.

3.7 Inhibition Mechanism

Figure 8 shows the dependence of inhibition efficiency of 10^{-3} M concentrations of compounds I, II, and III on exposure time. Some features could be recognized in the curves of Fig. 8. Firstly, the inhibition efficiency increases in the order: I > II > III. Secondly, the dependence of inhibition efficiency on exposure time increases in the reverse order: III > II > I. These observations could be interpreted in view of the number of ethylene oxide units contained in the molecular structures of the surfactants. The higher the number of ethylene oxide units, the higher the surface area covered by the adsorbed molecules, and thus the higher is the inhibition efficiency. On the other hand, the higher the number of ethylene oxide units, the shorter the time needed to reach the maximum possible inhibition efficiency and hence the less-dependent inhibition efficiency on time.

On the other hand, electrochemical experiments suggested a mixed-type inhibitor mechanism. Thus, the compound molecules adsorb at both anodic and cathodic sites on the steel surface. The adsorbed molecules construct a film that suppress both the anodic and cathodic half-reactions by preventing the transfer of mass and charge between the steel and the corrosive environment.

Gemini surfactants have unique molecular structure which differs from that of the ordinary surfactant molecule with just

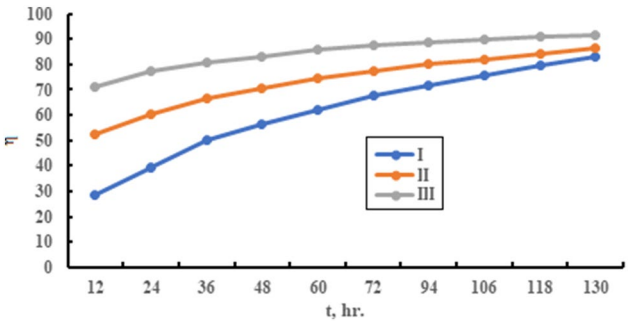

Fig. 8 Relationship between inhibition efficiency and exposure time in 0.1 M HCl solutions containing 10^{-3} M of compounds I, II, and III

hydrophilic head and a hydrophobic tail. It could be seen in the present surfactants that the oxygen atoms as well as nitrogen atoms with their lone pairs of electrons spread almost everywhere in their molecular structure. Since the adsorption process is achieved through these lone pair electrons, the surfactant molecules are adsorbed more likely in a horizontal manner. In such adsorption mode, the adsorbed molecule covers a surface area of the steel much higher than that expected if it adsorbs vertically. This postulated mode of adsorption is confirmed by the calculated values of A_{min} presented in Table 1. According to this argument, just small concentrations are needed to reach the maximum attainable capacity of inhibition, as obtained from the corrosion measurement techniques.

4 Conclusions

- The three tested Gemini surfactants act as good corrosion inhibitor for acid corrosion of carbon steel.
- The inhibition efficiency increases with increasing surfactant concentration, the number of propylene oxide units, and exposure time.
- The surfactants were found to be mixed-type inhibitors. They inhibit the steel corrosion via horizontal adsorption of their molecules on both anodic and cathodic sites at the steel surface.
- The adsorption process is spontaneous and follows Langmuir isotherm.

Table 5 AFM roughness data of investigated compounds (A–B) at 300 ppm for 1 day at 25 °C

	Free acid	I	II	III
Area (pm^2)	100.8	100.8	100.8	100.8
S_a (nm)	978.76	317.25	272.8	238.85
S_p (nm)	2710.1	1114.8	1030.7	779.81
S_v	− 5.0681 µm	− 2177.1 nm	− 1261.6 nm	− 891.71 nm

Compliance with Ethical Standards

Conflict of interest The authors declare that they have no conflict of interest.

References

1. El Bakri Y, Guo L, Essassi EM (2019) Electrochemical, DFT and MD simulation of newly synthesized triazolotriazepine derivatives as corrosion inhibitors for carbon steel in 1 M HCl. J Mol Liq 274:759–769
2. El-Etre A, Tantawy AH, Eid S, Seyam DF (2017) Research article open access corrosion inhibition of aluminum by novel amido-amine based cationic surfactant in 0.5 M HCl solution. J Basic Environ Sci 2:128–139
3. Erami RS, Amirnasr M, Meghdadi S, Talebian M, Farrokhpour H, Raeissi K (2019) Carboxamide derivatives as new corrosion inhibitors for mild steel protection in hydrochloric acid solution. Corros Sci 151:190–197
4. Fouda AS, El-Hady El-Maksoud SA, Belal AAM, El-Hossiany A, Ibrahium A (2018) Effectiveness of some organic compounds as corrosion inhibitors for stainless steel 201 in 1 M HCl: experimental and theoretical studies. Int J Electrochem Sci 13:9826–9846
5. Goyal M, Kumar S, Bahadur I, Verma C, Ebenso EE (2018) Organic corrosion inhibitors for industrial cleaning of ferrous and non-ferrous metals in acidic solutions: a review. J Mol Liq 256:565–573
6. Likhanova NV, Arellanes-Lozada P, Olivares-Xometl O, Hernández-Cocoletzi H, Lijanova IV, Arriola-Morales J, Castellanos-Aguila J (2019) Effect of organic anions on ionic liquids as corrosion inhibitors of steel in sulfuric acid solution. J Mol Liq 279:267–278
7. Mulyaningsih N (2019) Influence of organic corrosion inhibitor on corrosion behavior of St-37 carbon steel in NaCl medium. AIP Conf Proc 1:030008
8. Nguyen DT, To HTX, Gervasi J, Gonon M, Olivier M-G (2018) Corrosion inhibition of carbon steel by hydrotalcites modified with different organic carboxylic acids for organic coatings. Prog Org Coat 124:256–266
9. Popoola LT (2019) Organic green corrosion inhibitors (OGCIs): a critical review. Corros Rev 37(2):71–102
10. Quraishi MA, Chauhan DS, Saji VS (2020) Heterocyclic organic corrosion inhibitors: principles and applications. Elsevier, New York
11. Verma C, Ebenso EE, Quraishi M (2020) Molecular structural aspects of organic corrosion inhibitors: influence of –CN and –NO_2 substituents on designing of potential corrosion: inhibitors for aqueous media. J Mol Liq 316:113874
12. Verma C, Haque J, Quraishi M, Ebenso EE (2019) Aqueous phase environmental friendly organic corrosion inhibitors derived from one step multicomponent reactions: a review. J Mol Liq 275:18–40
13. Xhanari K, Finšgar M (2019) Organic corrosion inhibitors for aluminum and its alloys in chloride and alkaline solutions: a review. Arab J Chem 12(8):4646–4663
14. El Faydy M, Lakhrissi B, Jama C, Zarrouk A, Olasunkanmi LO, Ebenso EE, Bentiss F (2020) Electrochemical, surface and computational studies on the inhibition performance of some newly synthesized 8-hydroxyquinoline derivatives containing benzimidazole moiety against the corrosion of carbon steel in phosphoric acid environment. J Mater Res Technol 9(1):727–748
15. Cherrak K, Benhiba F, Sebbar N, Essassi E, Taleb M, Zarrouk A, Dafali A (2019) Corrosion inhibition of mild steel by new benzothiazine derivative in a hydrochloric acid solution: experimental evaluation and theoretical calculations. Chem Data Collect 22:100252
16. Luo X, Ci C, Li J, Lin K, Du S, Zhang H, Li X, Cheng YF, Zang J, Liu Y (2019) 4-Aminoazobenzene modified natural glucomannan as a green eco-friendly inhibitor for the mild steel in 0.5 M HCl solution. Corros Sci 151:132–142
17. Aiad I, Shaban SM, Elged AH, Aljoboury OH (2018) Cationic surfactant based on alginate as green corrosion inhibitors for the mild steel in 1.0 M HCl. Egypt J Pet 27(4):877–885
18. Ayukayeva VN, Boiko GI, Lyubchenko NP, Sarmurzina RG, Mukhamedova RF, Karabalin US, Dergunov SA (2019) Polyoxyethylene sorbitan trioleate surfactant as an effective corrosion inhibitor for carbon steel protection. Colloids Surf A 579:123636
19. Fouda A, Zaki E, Khalifa M (2019) Some new nonionic surfactants based on propane tricarboxylic acid as corrosion inhibitors for low carbon steel in hydrochloric acid solutions. J Bio Tribo Corros 5(2):1–15
20. Negm NA, El Hashash MA, Abd-Elaal A, Tawfik SM, Gharieb A (2018) Amide type nonionic surfactants: synthesis and corrosion inhibition evaluation against carbon steel corrosion in acidic medium. J Mol Liq 256:574–580
21. Shaban SM, Aiad I, Moustafa AH, Aljoboury OH (2019) Some alginates polymeric cationic surfactants; surface study and their evaluation as biocide and corrosion inhibitors. J Mol Liq 273:164–176
22. Han T, Guo J, Zhao Q, Wu Y, Zhang Y (2020) Enhanced corrosion inhibition of carbon steel by pyridyl Gemini surfactants with different alkyl chains. Mater Chem Phys 240:122156
23. Khalaf MM, Tantawy AH, Soliman KA, Abd El-Lateef HM (2020) Cationic Gemini-surfactants based on waste cooking oil as new 'green' inhibitors for N80-steel corrosion in sulphuric acid: a combined empirical and theoretical approaches. J Mol Struct 1203:127442
24. Pakiet M, Tedim J, Kowalczyk I, Brycki B (2019) Functionalised novel Gemini surfactants as corrosion inhibitors for mild steel in 50 mM NaCl: experimental and theoretical insights. Colloids Surf A 580:123699
25. Yousefi A, Javadian S, Sharifi M, Dalir N, Motaee A (2019) An experimental and theoretical study of biodegradable Gemini surfactants and surfactant/carbon nanotubes (CNTs) mixtures as new corrosion inhibitor. J Bio Tribo Corros 5(4):82
26. Zhou T, Yuan J, Zhang Z, Xin X, Xu G (2019) The comparison of imidazolium Gemini surfactant [$C_{14\text{-}4}$–C_{14}im] Br_2 and its corresponding monomer as corrosion inhibitors for A3 carbon steel in hydrochloric acid solutions: experimental and quantum chemical studies. Colloids Surf A 575:57–65
27. Jingnan C, Wei L (2018) Lipophilization of phenolic acids through esterification using *p*-toluenesulfonic acid as catalyst. Grain Oil Sci Technol 1(2):91–96
28. Ouellette RJ, David Rawn J (2018) In: Ouellette RJ, David Rawn (eds) Organic chemistry, 2nd edn. Academic. https://doi.org/10.1016/B978-0-12-812838-1.50022-0
29. Liu M-M, Mei Q, Zhang Y-X, Bai P, Guo X-H (2017) Palladium-catalyzed amination of chloro-substituted 5-nitropyrimidines with amines. Chin Chem Lett 28(3):583–587
30. Ahmadova GA, Abilova AZ, Rahimov RA, Asadov ZH, Ahmadbayova SF (2018) Influence of head-group composition and (chloro) propoxy units disposition consequency on properties of surfactants based on lauric acid, propylene oxide, epichlorohydrin and ethanolamines. Mater Chem Phys 205:416–422
31. Asadov ZH, Ahmadova GA, Rahimov RA, Abilova AZ, Zargarova SH, Zubkov FI (2018) Synthesis and properties of quaternary ammonium surfactants based on alkylamine, propylene oxide, and 2-chloroethanol. J Surfactants Deterg 21(2):247–254

32. Sheng Y, Wu X, Lu S, Li C (2016) Experimental study on foam properties of mixed systems of silicone and hydrocarbon surfactants. J Surfactants Deterg 19(4):823–831
33. Pinazo A, Pons R, Bustelo M, Manresa MÁ, Moran C, Raluy M, Pérez L (2019) Gemini histidine based surfactants: characterization; surface properties and biological activity. J Mol Liq 289:111156
34. Pisárčik M, Pupák M, Devínsky F, Almásy L, Tian Q, Bukovský M (2016) Urea-based Gemini surfactants: synthesis, aggregation behaviour and biological activity. Colloids Surf A 497:385–396
35. Abd-Elaal AA, Elbasiony N, Shaban SM, Zaki E (2018) Studying the corrosion inhibition of some prepared nonionic surfactants based on 3-(4-hydroxyphenyl) propanoic acid and estimating the influence of silver nanoparticles on the surface parameters. J Mol Liq 249:304–317
36. Hegazy M, El-Etre A, El-Shafaie M, Berry K (2016) Novel cationic surfactants for corrosion inhibition of carbon steel pipelines in oil and gas wells applications. J Mol Liq 214:347–356
37. Chen G, Yan J, Liu Q, Zhang J, Li H, Li J, Qu C, Zhang Y (2019) Preparation and surface activity study of amino acid surfactants. C R Chim 22(4):277–282

Publisher's Note Springer Nature remains neutral with regard to jurisdictional claims in published maps and institutional affiliations.